

AD-A158 825

OPTICAL/INFRARED PROPERTIES OF ATMOSPHERIC AEROSOLS
WITH AN IN-SITU MULTI. (U) FAME ASSOCIATES INC FORT
COLLINS CO J B WEDDING ET AL. APR 85 FA-AF-14385

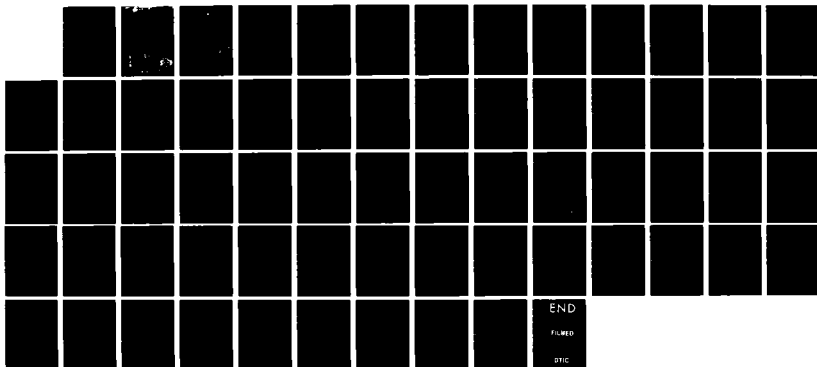
1/1

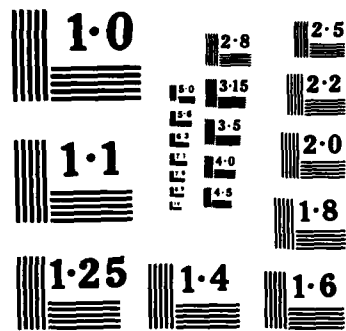
UNCLASSIFIED

AFOSR-TR-85-0586 F49620-84-C-0101

F/G 17/8

NL





NATIONAL BUREAU OF STANDARDS
MICROCOPY RESOLUTION TEST CHART

AD-A158 825

Optical/Infrared Properties of Atmospheric
Aerosols with an In-Situ, Multi-Wavelength,
Multichannel Nephelometer System: Phase I

AEROSOL SCIENCE LABORATORY

DIRECTOR, JAMES B. WEDDING, PH.D.

FARE ASSOCIATES, INC.
FLUID & AEROSOL MECHANICS ENGINEERS
POST OFFICE BOX 572
FORT COLLINS, COLORADO 80521

FILE COPY

DTIC
S
D

8 21 154

Approved for public release
Distribution unlimited.



Aerosol Science Laboratory
Director, James B. Wedding, Ph.D.

FAME ASSOCIATES, INC.
Fluid & Aerosol Mechanics Engineers

Post Office Box 572
Fort Collins, Colorado 80522
Phone (303) 221-0678

Optical/Infrared Properties of Atmospheric
Aerosols with an In-Situ, Multi-Wavelength,
Multichannel Nephelometer System: Phase I

Final Report
Contract #F49620-84-C-0101

Submitted to:

Lt. Col. Gerald J. Dittberner
AFOSR
Directorate of Chemical and Atmospheric Sciences
Building 410
Bolling AFB, DC 20332-6448

Prepared by:

James B. Wedding, Young J. Kim, and
Michael A. Weigand

DTIC
ELECTE
AUG 29 1985
S **D**
G

DISTRIBUTION STATEMENT A

Approved for public release
Distribution Unlimited

30 April 1985

AIR FORCE OFFICE OF SCIENTIFIC RESEARCH (AFOSR)
NOTICE OF REVISION
This report is the property of the Air Force Office of Scientific Research (AFOSR) and is loaned to you. It and its contents are not to be distributed outside your organization.
Approved for public release
Distribution Unlimited
MATTHEW J. ...
Chief, Technical Information Division

Unclassified

SECURITY CLASSIFICATION OF THIS PAGE (When Data Entered)

REPORT DOCUMENTATION PAGE		READ INSTRUCTIONS BEFORE COMPLETING FORM
1. REPORT NUMBER AFOSR-TR- 35-0506	2. GOVT ACCESSION NO. AD-A158825	3. RECIPIENT'S CATALOG NUMBER
4. TITLE (and Subtitle) Optical/Infrared Properties of Atmospheric Aerosols with an In-Situ, Multi-Wavelength Multichannel Nephelometer System: Phase I		5. TYPE OF REPORT & PERIOD COVERED Final 15 Sept 84 ~ 14 Mar 85
		6. PERFORMING ORG. REPORT NUMBER FA-AF-14385
7. AUTHOR(s) James B. Wedding, Young J. Kim, and Michael A. Weigand		8. CONTRACT OR GRANT NUMBER(s) F49620-84-C-0101
9. PERFORMING ORGANIZATION NAME AND ADDRESS FAME Associates, Inc. P. O. Box 572 Fort Collins, CO 80522		10. PROGRAM ELEMENT, PROJECT, TASK AREA & WORK UNIT NUMBERS 65802F 3005/A1
11. CONTROLLING OFFICE NAME AND ADDRESS Air Force Office of Scientific Research Building 410 Bolling AFB, DC 20332		12. REPORT DATE April 1985
		13. NUMBER OF PAGES 56
14. MONITORING AGENCY NAME & ADDRESS (if different from Controlling Office)		15. SECURITY CLASS. (of this report) Unclassified
		15a. DECLASSIFICATION/DOWNGRADING SCHEDULE
16. DISTRIBUTION STATEMENT (of this Report) Unlimited Approved for public release; distribution unlimited.		
17. DISTRIBUTION STATEMENT (of the abstract entered in Block 20, if different from Report)		
18. SUPPLEMENTARY NOTES		
19. KEY WORDS (Continue on reverse side if necessary and identify by block number) Nephelometer; Differential Scattering; Atmospheric Aerosols; Infrared; In-Situ Measurement; Nonspherical Particles		
20. ABSTRACT (Continue on reverse side if necessary and identify by block number) There exists a need to develop new instrumentation which can provide an in-situ, real time measurement of the total differential scattering patterns from individual airborne particles of different composition and shape under natural and man-made atmospheric conditions. During the Phase I study, a literature survey was conducted, system requirements developed for an in-situ, multi-wavelength, multichannel nephelometer system, and technical feasibilities were investigated. Finally, design parameters		

Unclassified

SECURITY CLASSIFICATION OF THIS PAGE(When Data Entered)

of the nephelometer system including the particle sampling inlet, the optical system, and the data acquisition system were optimized. The proposed nephelometer system will measure the differential scattering patterns of individual aerosol particles at three laser wavelengths, in three scattering planes. Successful development of such an instrument during the Phase II efforts will assist in filling the void of knowledge of the optical/infrared properties of atmospheric aerosols and their interactions with electromagnetic radiation fields.

Accession For	
NTIS GRA&I	<input checked="" type="checkbox"/>
DTIC TAB	<input type="checkbox"/>
Unannounced	<input type="checkbox"/>
Justification	
By _____	
Distribution/	
Availability Codes	
Dist	Avail and/or Special
A/1	



Unclassified

SECURITY CLASSIFICATION OF THIS PAGE(When Data Entered)

Table of Contents

	Page #
Cover Sheet	i
List of Tables	iv
List of Figures	v
1.0 Statement of the Problem	1
2.0 Phase I Objectives	6
2.1 Phase I Technical Objectives	6
2.2 Phase I Task Implementation	6
3.0 Summary of Phase I Research Work	8
3.1 Literature Survey	8
3.2 Principles and Constituents Pertaining to the Characterization of the Optical Properties of Aerosols	9
3.3 Development of System Requirements	10
3.4 Optimization of the Design Parameters	11
4.0 Results of Phase I Research	14
4.1 Review of Light Scattering Theories and Scattering Calculations	14
4.2 Particle Sampling System	25
4.3 Optical System	31
4.4 Data Acquisition System	44
5.0 Potential Post Application	48
5.1 Potential Commercial Applications	48
5.2 Potential Use by the Federal Government	50
6.0 Conclusions	52
7.0 Participating Professional Personnel	54
References	55

List of Tables

Table		Page #
1	Q _{scat} Calculation for $\lambda = 0.6328 \mu\text{m}$	23
2	Q _{scat} Calculation for $\lambda = 1.06 \mu\text{m}$	23
3	Q _{scat} Calculation for $\lambda = 3.39 \mu\text{m}$	24
4	Q _{scat} Calculation for $\lambda = 10.6 \mu\text{m}$	24
5	Total Radiant Flux Scattered by a Single Particle	35
6	Range of Expected Power Incident on a Detector at $0^\circ \sim 180^\circ$ Scattering Angles	35
7	Typical Specifications of Detectors	43

List of Figures

Figure		Page #
1	Angular Scattering by Spheres with $m = 1.55$; the incident light is polarized parallel (- - -) or perpendicular (——) to the scattering plane	17
2	Imaginary part of the refractive index of several solids and liquids that are found as atmospheric particles	22
3	Wedding PM Inlet for the Dichotomous Sampler 10	28
4	Effectiveness Curve for the Wedding PM Inlet 10	29
5	Particle Sampling System	30
6	Optical System	40
7	Data Acquisition System	46

1.0 Statement of the Problem

Recent developments in electro-optical and infrared technologies have brought a new dimension in various areas of civil and military applications. Laser beams or broadband infrared radiation has been used in remote sensing, thermal imaging, night vision devices, seeker/guidance, optical communication, designator, rangefinder, and directed energy weapon systems. Optical countermeasures such as obscurant smokes have also been developed. Such electro-optical and infrared systems have to detect/send electromagnetic energy from/to a target at a distance through the atmosphere. A major problem with EO/IR systems is that performance of those systems is greatly affected by both natural and man-made atmospheric conditions.

When an electromagnetic wave propagates through the atmosphere, it experiences both linear and nonlinear effects such as gaseous and aerosol absorption and scattering, turbulence, thermal blooming, air breakdown, etc. Intensity of electromagnetic radiation is attenuated due to absorption and scattering by atmospheric gases and aerosol particles. This transmission loss due to absorption and scattering also causes reduction in contrast of the target against the background for optical or thermal imaging systems. Amount of beam attenuation depends upon beam wavelength, pathlength, and atmospheric conditions such as atmospheric gas concentration, water content, aerosol concentration, and aerosol size distribution. Therefore, realistic performance tests of EO/IR systems and obscurant countermeasures must include an accurate evaluation of atmospheric transmittance.

Atmospheric gases absorb selectively radiation of certain wavelengths depending on their molecular structures. McClatchey et al. [1] made a compilation of all absorption lines of the major atmospheric gases. Strong absorbing gases are water vapor, carbon dioxide and ozone. Other absorbing

gases are nitrous oxide, carbon monoxide and methane. Long-range infrared systems are generally operated at one of the atmospheric "windows" at 3-4 μm , 4.5-5 μm or 8-12 μm where transmission loss due to absorption by atmospheric gases are relatively low. The dominant mechanism causing transmission losses in the atmospheric windows is extinction by particles. Aerosol extinction is thus an important factor in determining transmission losses and it depends on particle size, refractive index, particle shape and beam wavelength. Millimeter waves have been used to avoid problems resulting from beam attenuation due to aerosol particles; fog, haze, etc. However, they are affected by attenuation due to larger size particles such as rain droplets and snow flakes.

There have been efforts to develop models which can calculate spectral transmittances under different meteorological and atmospheric conditions. A computer code, LOWTRAN [2], has been developed for calculating the transmittance and background radiance of the earth's atmosphere from 0.25 to 29.5 μm at moderate spectral resolution of 20 cm^{-1} . The HITRAN [3], which can calculate the high-resolution atmospheric transmittance of the laser beams, has been developed by personnel at the Air Force Geophysics Laboratory. Some other transmission models have also been developed. The Electro-Optical Systems Atmospheric Effects Library (EOSAEL) includes models and computer codes that aid the user in determining the effect of atmospheric and man-made obscuring agents on radiation transmission [4]. The greatest uncertainty in the application of computer models to the on-site calculation of the transmittance over optical paths is in the wavelength dependent attenuation of electromagnetic radiation by aerosol particles.

Aerosol attenuation becomes very important when an electro-optical or an infrared system is used under adverse atmospheric conditions such as at low visibility or when obscuring agent particles are present in the path. The capability

of predicting performance of such systems under various atmospheric conditions is essential for the system designer as well as the end user of such systems. It is necessary to characterize the optical properties of individual aerosol particles in order to predict performance of optical and infrared systems.

Particles present in the earth's environment from the surface boundary layer to orbital altitudes, which affect performance of optical and infrared systems, range from natural and artificial atmospheric aerosols through cloud droplets and meteoric dust. Hygroscopic aerosol such as cloud, fog, and haze droplets can be considered as spherical in their shape. Much of the atmospheric aerosols which originate from soil, salt, or pollen, artificially obscurant particles, ice clouds, and interplanetary or meteoric dust in the upper atmosphere are known to be irregularly shaped. Quantitative analyses of scattering by atmospheric aerosols are limited by the fact that little information is available about the complex index of refraction. Refractive index of particles is a function of particle composition and beam wavelength. No exact solution for irregularly shaped particles scattering is available at present. Therefore, it can be concluded that well-structured experiments to measure the light scattering pattern of individual particles are a better way of characterizing the optical properties of airborne particles.

Four different approaches have been used to date to characterize the optical properties of aerosol particles: remote measurement, analysis of collected samples, inferring optical constants from theoretical calculations, and in-situ measurement. Multichannel solar radiometry and Lidar are examples of remote measurements of the optical properties of aerosols. Particles collected on filters can often be examined by electron or light microscopy to obtain their size and shapes. Absorption by the collected particles can be measured using integrating plate [5] or diffusing plate [6] methods.

Scattering and absorption cross sections can be calculated using Mie's scattering theory [7,8] for spherical particles from the particle size distribution data measured with an optical particle sizing instrument. However, this approach has limitations resulting from measurement error due to uncertainties in particle refractive index and particle shape. Various in-situ measurement methods for characterizing the optical properties of atmospheric aerosols have been developed. In-situ measurement techniques can be classified into two types: those which measure on a large number of particles simultaneously and those which measure on individual particles one at a time. The former type includes transmissometer, nephelometer, extincitometer, and photoacoustic method. Measurements on ensemble of particles result in some kind of average quantities for a mixture containing particles whose optical properties and composition might be quite different. Since the advent of high-power collimated lasers, many measurements on differential scattering of single particles have been published. They usually take one of two approaches: levitate the particles in the scattering volume using an electric field or radiation pressure, or make rapid measurements with a rotating aperture/detector or an array of fixed detectors.

To completely describe the optical properties of non-spherical particles, one necessarily needs to quantify all elements of the Mueller matrix [7]. This matrix relates the intensity, polarization and phase state of light incident upon a particle to those of light scattered, transmitted or reflected by a particle. Simultaneous measurement of all sixteen Mueller matrix elements is considered as one approach which can give information concerning size, shape and chemical/biological properties of the scattering particles. Some successful measurements of the Mueller matrix elements have been reported [9]. However, this method needs further improvements in theory and experimental techniques in order to provide rapid particle-by-particle analysis of the

irregularly shaped particles [10]. Even if one could measure simultaneously in a short period of time all sixteen elements, the resulting data are extremely difficult to apply.

The normalized angular scattering pattern, the so-called phase function, is an important parameter to quantify in predicting the particles' effect on performance of EO/IR systems. The measured phase function can also be correlated to the physical/chemical characteristics of aerosol particles. Scattering pattern of a nonspherical particle can be no longer symmetric along the azimuthal directions. This necessitates that scattering measurements must be made simultaneously at different directions, ideally over the 4π steradians sphere. Refractive index of a particle changes with the wavelength of the incident beam. Thus, the phase function need be measured at different wavelengths, especially in the atmospheric window regions. There exists a need to develop a new instrument which can provide a real-time, in-situ, spectral measurements of scattering characteristics of individual atmospheric particles of different shape and composition.

Our proposed approach is to measure and record the multi-wavelength, angular distribution, in three different scattering planes, of the scattered light from individual particles passing through the small scattering volume. All measurements have to be done in a real-time manner without altering sample integrity or the physical/optical properties of the particles. During Phase I efforts, a literature survey has been conducted, system requirements have been developed, technical feasibility of the developed concept has been investigated, and the design parameters have been optimized.

2.0 Phase I Objectives & Statement of Work

2.1 Phase I Technical Objectives

The specific objective of Phase I work were as follows:

- a. The design parameters were to be identified and optimized for a new multi-wavelength, multichannel nephelometer system, which includes the sampling inlet, the optical system and the data acquisition system, capable of in-situ, real-time measurement of differential scattering patterns of individual aerosol particles.
- b. The technical feasibility of the developed system concept was to be investigated.
- c. Using state-of-the-art techniques, a prototype system was to be designed.

2.2 Phase I Task Implementation

The Phase I research contract, #F49620-84-C-0101, delineates specific tasks and schedules as follows:

1) Section B, 0001 RESEARCH

0001AA The contractor will:

- a. Conduct a literature survey pertaining to measurement of optical properties of aerosol.
- b. Investigate the principles and constraints pertaining to the characterization of the optical properties of aerosols.
- c. Develop system requirements for determination of optical properties.
- d. Optimize the design parameters for the proposed multi-wavelength, multi-channel nephelometer system including the sampling inlet, the optical system and the data acquisition system.

2) Section B, 0002 REPORTS

Reports identified below shall be prepared in accordance with Exhibit A and delivered in accordance with Section F.

0002AA Final Report.

3) SECTION F.1, Period of Performance and Delivery

The supplies and services shall be delivered or performed during the following period:

0001AA 15 September 1984 through 14 March 1985

0002AA FINAL REPORT DUE 13 May 1985

3.0 Summary of Phase I Research Work

All objectives of Phase I work have been accomplished successfully. Our literature survey showed a need for better understanding of optical properties of atmospheric and man-made aerosol particles. Upon completion of the Phase I research, we have concluded that development of the proposed multi-wavelength, multichannel nephelometer system is technically feasible using state-of-the-art techniques. Successful development of such a system will provide valuable informations in broad areas of potential applications such as design and performance analysis of electro-optical and infrared systems, remote sensing, modeling atmospheric transmission of optical/infrared radiations, optical or thermal imaging through a horizontal or slant path, optical countermeasures, CB agent detection, direct energy weapon system, optical communication, radiation transfer in the earth's atmosphere, air quality and visibility monitoring, combustion analysis, process engineering, flow cytometric analysis, multi-phase flows analysis, etc.

A brief summary of each task performed during Phase I work is presented as follows:

3.1 Literature Survey

Existing literature related to measurement of optical properties of aerosols has been reviewed through various technical journals and government publications. Upon completion of literature survey, it is concluded that a new instrument, which can provide a fast-response, in-situ, spectral measurement of scattering characteristics of individual aerosol particles, needs to be developed for better understanding of optical properties of atmospheric aerosols and their effects on the performance of electro-optical and infrared systems. It is found that no nephelometer system developed to date has capability of fulfilling such measurement requirements. Relatively little work has been directed toward

in-situ, real-time measurement of scattering characteristics of individual aerosol particles. Most of the experimental work on scattering characteristics of aerosols have used a nephelometer in acquiring data for ensemble of randomly oriented particles instead of a single particle. All differential scattering measurements to date on single particles have been made in one scattering plane, at one visible wavelength, and at relatively low measurement speeds.

Besides measurement techniques of optical properties of aerosols, literature survey on other related areas such as scattering theories for particles of different shape and composition, aerosol sampling techniques and optical particle sizing has also been performed.

3.2 Principles and Constraints Pertaining to the Characterization of the Optical Properties of Aerosols

Absorption and scattering by aerosols are the main mechanisms which affect the performance of electro-optical and infrared systems under natural and man-made atmospheric conditions. Theoretical background and measurement techniques pertaining to the characterization of the optical properties of aerosols have been reviewed.

Four different approaches have been used to measure the optical properties of atmospheric aerosols: 1) remote measurement (solar extinction and bistatic lidar), 2) collected samples (absorption and diffusion), 3) inferring optical constants from theoretical analysis, and 4) in-situ measurement (nephelometer, transmissometer, and photoacoustic method). Principles and constraints of each of those methods have been investigated.

Scattering characteristics of aerosols, which depend on particle size, incident beam wavelength, refractive index, particle shape and orientation, are more complicated and important quantities requiring attention in many areas of applications. Nephelometers which measure directly the scattering characteristics of individual particles or an ensemble of particles in the scattering volume can be classified into three types based on their optical configuration; fixed-angle nephelometers, integrating nephelometers, and polar nephelometers. Principles and constraints of each of the three types of nephelometers have also been investigated.

A system concept for a new nephelometer system capable of in-situ, real-time, multi-wavelength measurement of the scattering characteristics of individual airborne particles of different shape and composition has been developed.

3.3 Development of System Requirements

System requirements for the proposed in-situ, multi-wavelength, multichannel nephelometer system have been determined as follows:

- 1) Particle size range; -0.3 to 20 μm in diameter for equivalent spherical particles
- 2) Particle shape; -spherical or nonspherical particles
- 3) Measurement angle; - $5^\circ \sim 175^\circ$ in three different scattering planes
- 4) Particle concentration; - $\leq 10^5$ particles/cc
- 5) Particle refractive index; -non-absorbing or absorbing
- 6) Particle sampling system; -minimize size biasing during particle sampling
 -provide single particle measurement

- 7) Measurement wavelengths; -three laser wavelengths (0.6328, 3.39 and 10.6 μ m)
- 8) Measurement speed; - \leq 100 particles/sec
- 9) Measurement accuracy; -better than \pm 10% in forward directions
- 10) Scattering intensity measurement; -two polarization components perpendicular and parallel to the scattering plane
- 11) Data representation; -store and analyze the measured data with a computer based fast data acquisition system
-provides real-time, in-situ measurement
- 12) Power requirement; -110 VAC, 60Hz
- 13) Environmental requirement; -laboratory and field operable

3.4 Optimization of the Design Parameters

Technical feasibilities of the developed system concept to satisfy the system requirements have been investigated. Based on the results of technical feasibility study, an in-situ, multi-wavelength, multichannel nephelometer system including the sampling inlet, the optical system and the data acquisition system has been designed.

a. Sampling Inlet

The particle sampling system shall sample airborne particles and direct them through the scattering volume of the receiving optics with minimal size biasing. Wedding PM₁₀ inlet for a dichotomous sampler initially developed for monitoring ambient particulate matter shall be used as a sampling inlet for the proposed nephelometer system. Effectiveness of the Wedding PM₁₀ inlet had been well characterized

previously through a series of wind tunnel tests [11]. It has D_{50} value, associated with a 50% effectiveness value, of $10.7 \mu\text{m}$ and samples aerosol particles at a flow rate of 16.67 lpm with minimal dependence on wind speed and wind direction. The inlet employs a unique, omnidirectional cyclone fractionator. In dynamic tests with solid particles, the inlet displayed no particle-bounce problem. A schematic of the particle sampling system is shown in Figure 5 in Section 4.2.

b. Optical System

Feasibilities of various optical configurations developed for single particle differential scattering measurements have been investigated. Theoretical calculations on the expected signal power levels incident on detectors have been performed to determine the measurement limits of the proposed nephelometer. Lower limit of measurement size range of the nephelometer design was determined as $0.3 \mu\text{m}$ for visible wavelength and $1.0 \mu\text{m}$ for infrared wavelengths. An optical system employing ellipsoidal reflectors and rotating apertures has been designed for the proposed nephelometer. A schematic of the optical system is shown in Figure 6 in Section 4.3. Three laser beams are focused on the primary focal points of circular strips of ellipsoidal reflectors. Scattered light beams are reflected by the ellipsoidal reflectors and directed onto detectors located at the secondary focal points of the ellipsoidal reflectors. Rotating apertures are placed in front of detectors to make a complete scan of angular distribution of scattered light over 2 degrees. A more complete discussion of the optical system is presented in Section 4.3.

c. Data Acquisition System

A fast response, microcomputer-based data acquisition system, which can acquire the measured differential scattering data and store them simultaneously into a mass storage device, has been designed. A schematic of the data acquisition system is shown in Figure 7 in Section 4.4. Simultaneous sample and hold technique is employed to sample all nine detector channels in a very short time interval of ± 5 nanoseconds in order to measure scattered intensities corresponding to the same scattering angle. The data acquisition system based on an LSI-11/23 computer is capable of analog inputs acquisition and continuous analog throughput to or from disk at up to 250,000 samples/sec. Measured data are stored into a hard disk in a real-time manner and transferred later to a 60 Mbytes cartridge tape drive for permanent back-up storage. The data acquisition system includes detector preamplifiers, signal conditioning electronics, a simultaneous S & H circuit, an A/D converter, buffers, a computer, disk drives, a video terminal, a printer, and a tape drive. Capabilities of the data acquisition system is further discussed in Section 4.4.

4.0 Results of Phase I Research

4.1 Review of Light Scattering Theories and Scattering Calculations

1) Scattering by Spherical Particles

The scattering of an electromagnetic wave by an arbitrarily shaped particle is usually described using the Stokes vector [7]:

$$\begin{pmatrix} I_{1s} \\ I_{2s} \\ U_s \\ V_s \end{pmatrix} = \frac{\lambda^2}{4\pi^2 R^2} S_{ij} \begin{pmatrix} I_{1o} \\ I_{2o} \\ U_o \\ V_o \end{pmatrix} \quad (1)$$

Index o characterizes the incident radiation, index s is the scattered radiation, λ is the wavelength, while R is the distance between the scattering particle and detector. S_{ij} are the elements of the 4 X 4 Mueller matrix. I_1, I_2, U and V are the Stoke's parameters. All the components in the Mueller matrix are functions of the scattering angle, the wavelength of the incident beam, and the particle size, shape, orientation, and complex index of refraction. Light plane polarized parallel to the plane of scattering has Stokes vector (1,0,0,0); and light plane polarized perpendicular to the plane of scattering has Stokes vector (0,1,0,0). The element U and V characterize elliptical polarization. Symmetry conditions can simplify the Mueller matrix. For randomly oriented particles, Perrin [12] has shown that the number of independent elements reduces to six.

For a single spherical particle, the Mueller Matrix is further reduced to

$$\begin{bmatrix} I \\ I_{1s} \\ I_{2s} \\ U \\ S \\ V \\ S \end{bmatrix} = \frac{\lambda^2}{4\pi^2 R^2} \begin{vmatrix} S_{11} & 0 & 0 & 0 \\ 0 & S_{22} & 0 & 0 \\ 0 & 0 & S_{33} & S_{34} \\ 0 & 0 & -S_{34} & S_{33} \end{vmatrix} \begin{bmatrix} I_{1o} \\ I_{2o} \\ U \\ V \\ 0 \end{bmatrix} \quad (2)$$

Mie [7] solved the Maxwell equations related to the scattering of light by a homogeneous dielectric spherical particle with the appropriate boundary conditions. According to the Mie theory, scattered light intensity for incident unpolarized light is

$$I(\theta) = \frac{\lambda^2}{4\pi^2 R^2} I_o \left(\frac{i_1(\alpha, m, \theta) + i_2(\alpha, m, \theta)}{2} \right) \quad (3)$$

where i_1 and i_2 are Mie intensity functions ($= |E_1|^2$ and $|E_2|^2$; E_1 and E_2 are complex variables); α is size parameter ($\alpha = \pi D/\lambda$); and m is complex refractive index of particle.

The dimensionless intensity functions i_1 and i_2 are proportional to the square of the electric field vectors perpendicular and parallel respectively, to the plane of the observed scattered beam. The Mie intensity functions are related to the Mueller elements as

$$\begin{aligned} S_{11} &= i_2 = |E_2|^2, & S_{22} &= i_1 = |E_1|^2 \\ S_{33} &= 1/2(E_2 E_1^* + E_1 E_2^*) \\ S_{34} &= i/2(E_2 E_1^* - E_1 E_2^*) \end{aligned} \quad (4)$$

For spherical particles, the values of S_{11} , S_{22} , S_{33} , and S_{34} can be computed using the computer code developed by Dave [13] once the particle diameter and refractive index are known.

The phase function, which is defined as the ratio of the energy scattered per unit solid angle in a given direction to the average energy scattered per unit solid angle in all directions, is an important parameter to describe the optical properties of aerosol particles. Scattering by particles that are very small when compared with the wavelength ($\alpha \ll 1$) is known as Rayleigh scattering. The Rayleigh phase function is given by [14]

$$P_R(\theta) = 0.75 (1 + \cos^2 \theta) \quad (5)$$

The Mie phase function is given by

$$P_m(\theta) = \frac{I(\theta)}{\frac{1}{4\pi} \int_0^{4\pi} I(\theta) d\Omega} = \frac{4\pi I(\theta)}{I_0 C_s} \quad (6)$$

where Ω is the solid angle and C_s is the scattering cross section of the particle. A plot of angular scattering by spheres with $m=1.55$ is shown in Figure 1 [15]. For small size parameters, the Rayleigh scattering patterns are obtained: perpendicularly polarized light is scattered isotropically, while light polarized parallel to the scattering plane vanishes at a scattering angle of 90° . The first deviations from Rayleigh theory appear as forward-backward asymmetry, with more light being scattered in forward directions. As the particle size is increased further, the asymmetry becomes more pronounced and the dominant forward scattering pattern is increased and more light is scattered into narrow forward directions for larger particles.

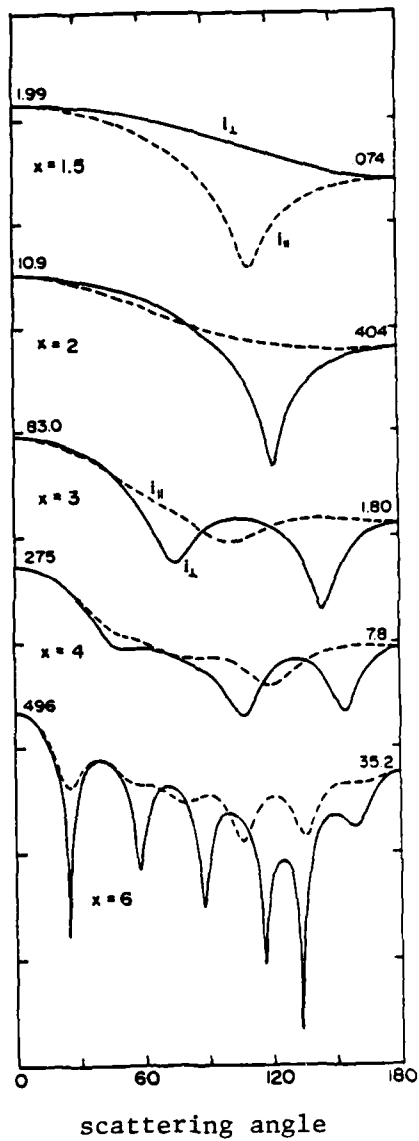


Figure 1
 Angular Scattering by Spheres with $m=1.55$; the incident light is polarized parallel (---) or perpendicular (—) to the scattering plane [15].

For very large spherical particles, the method of geometric optics is used as an alternative to the substantial quantity of computer time and memory required for a computation using Mie theory. The contribution of diffraction, reflection and refraction must be calculated and added to obtain the geometric phase functions [16].

2) Scattering by Non-Spherical Particles

No rigorous theory of scattering by irregularly shaped particles is available now and in all likelihood the situation will remain unchanged in the near future even with the advent of high speed computers with very large memory capacities. Some scattering theories have been developed for particles of particular shapes, which have a symmetry about one or more axes, including circular cylinders [17,18], spheroids [29,20], flat disks [21], fibrous particles [22,23] and aggregates of particles [24,25]. Various analytical and numerical techniques have been developed for the problem of scattering by arbitrarily shaped inhomogeneous particles such as: method of moment [26], perturbation method [27], point matching method [28], extended boundary condition method [29-31], and semi-empirical theory [32]. Various methods of calculating the light scattering properties of nonspherical particles have been reviewed by Schuerman [33] and Barber and Massoudi [34]. Each method has its own advantages and limitations and none of the above methods can yield accurate results for scattering by arbitrarily shaped inhomogeneous particles.

Instead of the theoretical solutions, empirical approaches, which are to model the scattering occurrences by non-spherical particles using equivalent shape (usually spherical) as standard, have been tried. Measurements of light scattering by numerous types of irregularly shaped particles [35-38] indicate that scattering in the near forward directions is similar to that of an ensemble of equivalent spheres. Microwave analog measurements of angular scattering patterns have been performed for randomly oriented polydisperse particles of different types: rough spheres, cubes, octahedrons, convex particles, concave particles and fluffy particles [39]. Similar measurements have been done for twenty-eight particles of different sizes and shapes by Schuerman et al. [40]. The measured data were compared with Mie calculations based on the spheres of equivalent volume or cross sectional area. Correspondence with prediction was good in the forward directions whereas significant differences occurred at medium scattering angles and towards backscattering. Angular scattering patterns of irregularly shaped particles, convex and concave particles, with the size parameters in the range of 1.9 to 5.9 were similar to that of spherical particles of equivalent volumes. For the larger particles whose size parameter varies from 5.9 to 17.8, deviations in scattering intensities occurred at medium scattering angles. The intensity enhancement observed for backscattering, which is a typical behavior for mixtures of dielectric spheres, is not observed for nonspherical particles [39].

Pollack and Cuzzi [32] made similar conclusions for randomly oriented, irregularly shaped particles. When their size parameter is less than 5, their phase functions closely resemble those of spheres of equal volume. For larger particles whose size parameter is larger than 5, the phase function of nonspherical particles is similar to that of their spherical counterparts at small scattering angles, but shows marked deviations at larger angles.

Hodkinson [35] summarized the scattering behavior of a single particle with nonspherical shape. For particles smaller than $\alpha = 0.3$, the simple Rayleigh scattering pattern, whose absolute intensities are about equal for particles of equal volume, is observed regardless of their shape. With particles larger than this, up to $\alpha = 1$, the forward lobe of the scattering pattern is determined by particle dimension along the direction of incidence and resembles the pattern of a sphere of that diameter. When $1 < \alpha < 5$ the scattering pattern is so complex that no generalization with Mie calculations can be made. For larger particles, when $\alpha > 5$, the scattering can be approximated with geometric optics. The angular spread of the forward lobe is determined by the transverse dimensions of the particles, as in Fraunhofer diffraction [41].

3) Scattering Calculations

Light scattering by particles depends upon not only particle size and shape but also refractive index. Refractive index of a particle is determined by its chemical composition and is a function of wavelength, too. Imaginary part of the refractive

atmospheric particles is shown in Figure 2 [15]. Except for carbon, there are two distinct spectral regions in which k is high for those materials: one in the infrared and the other in the ultraviolet, with a region of high transparency between. This fact necessitates a need to measure the optical properties of atmospheric aerosols at different wavelengths of interest. Phase function data measured at visible wavelength can not be used to predict and evaluate electro-optical systems' performance at infrared wavelengths. If particle size is known, complex refractive index of a particle can be determined from angular scattering data measured with a nephelometer system. The hatched region in Figure 2 shows the approximate values of k of atmospheric aerosols at visible wavelengths inferred by various remote-sensing techniques [42,43]. If we compare these values of k with those for individual constituents of the atmospheric aerosols, it seems clear that k determined remotely is some kind of average for a mixture containing a small amount of a strongly absorbing component such as carbon and much larger amounts of weakly absorbing components. The proposed nephelometer system measures optical properties of individual particles to get their real representative values.

Total scattering cross section values and angular distribution of scattered light at different laser wavelengths have been calculated for spherical particles of different size and refractive index in order to predict signal levels scattered into different angles and investigate their dependency on different

variables. A computer code developed by Bohren and Huffman [15] was used to calculate the scattering matrix elements at 9° to 180° with a 9° increment and the scattering efficient factor, Q_{scat} values. Values of parameters used in scattering calculations are:

wavelength: 0.442, 0.488, 0.6328, 1.06, 1.15, 3.39, and 10.6 μm

particle size: 0.3, 0.6, 1, 3, 6, 10, 20, and 25 μm

refractive index: $n = 1.33, 1.46, 1.55, 1.65$ and 1.90
 $(m=n-ik)$ $k = 0.0, 0.1, 0.01, \text{ and } 0.005$

Some results of Q_{scat} calculations are presented in Table 1-4.

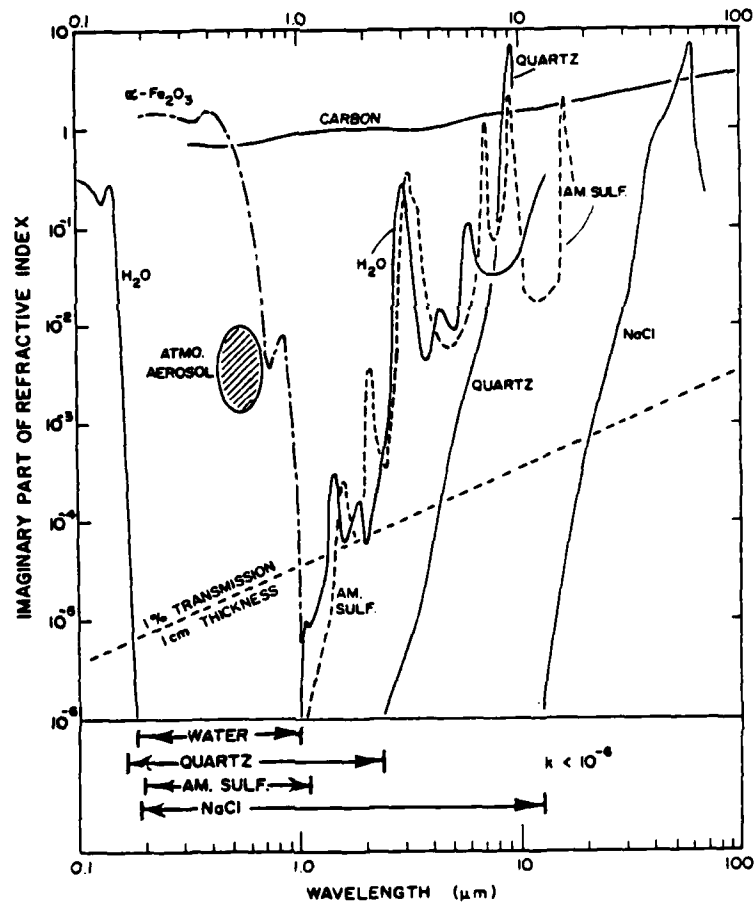


Figure 2
 Imaginary part of the refractive index of several solids and liquids that are found as atmospheric particles.

Table 1

Q Calculation for $\lambda = 0.6328 \mu\text{m}$
scat Q

Particle Diameter (μm)	Size Parameter	refractive index: $n=1.55$		
		$k=0.0$	$k=0.005$	$k=0.1$
0.3	1.489	0.9027	0.8949	0.7835
0.6	2.979	3.7014	3.6002	2.3306
1.0	4.965	3.6806	3.4745	1.8215
3.0	14.894	2.6513	2.2775	1.1888
6.0	29.788	2.0130	1.6023	1.1592
10.0	49.646	2.2356	1.5969	1.1513
20.0	99.292	2.0576	1.2749	1.1401
25.0	124.115	2.1201	1.2428	1.1368

Table 2

Q Calculation for $\lambda = 1.06 \mu\text{m}$
scat Q

Particle Diameter (μm)	Size Parameter	refractive index: $n=1.55$		
		$k=0.0$	$k=0.005$	$k=0.1$
0.3	0.889	0.1682	0.1678	0.1656
0.6	1.778	1.6359	1.6077	1.2311
1.0	2.964	3.7017	3.5998	2.3266
3.0	8.891	2.8473	2.5660	1.2531
6.0	17.783	2.1398	1.7838	1.1648
10.0	29.638	2.0366	1.6196	1.1593
20.0	59.275	2.0744	1.4292	1.1484
25.0	74.094	2.1348	1.3891	1.1447

Table 3

Q Calculation for $\lambda = 3.39 \mu\text{m}$
scat

Particle Diameter (μm)	Size Parameter	Q scat refractive index: $n=1.55$		
		$k=0.0$	$k=0.005$	$k=0.1$
0.3	0.278	0.001629	0.001630	0.001683
0.6	0.556	0.02644	0.82643	0.02704
1.0	0.927	0.1964	0.1959	0.1921
3.0	2.780	3.6771	3.5689	2.2741
6.0	5.560	2.7247	2.5692	1.4617
10.0	9.267	2.8636	2.5893	1.2749
20.0	18.534	2.0799	1.6983	1.1615
25.0	23.168	2.0906	1.7554	1.1635

Table 4

Q Calculation for $\lambda = 10.6 \mu\text{m}$
scat

Particle Diameter (μm)	Size Parameter	Q scat refractive index: $n=1.55$		
		$k=0.0$	$k=0.005$	$k=0.1$
0.3	0.089	0.0001693	0.00001693	0.00001751
0.6	0.178	0.0002715	0.0002715	0.0002807
1.0	0.296	0.002106	0.002106	0.002175
3.0	0.889	0.1682	0.1678	0.1656
6.0	1.778	1.6359	1.6077	1.2311
10.0	2.964	3.7017	3.5998	2.3266
20.0	5.928	2.3376	2.2100	1.3150
25.0	7.409	1.9281	1.7773	1.1064

4.2 Particle Sampling System

The particle sampling system must draw a sample of atmospheric aerosols with minimal size biasing and direct them in a train of single particles into the scattering volume of the system optics. Most of the optical instruments developed to date, including the nephelometer and optical particle counter, use a sampling tube as a particle sampling inlet. This type of sampling inlet is known to be ineffective because of its wind speed dependency and particle loss to the tube wall [44]. To obtain a representative measurement for particles present, one must draw a sample containing the particle size range of interest through an inlet device into the scattering volume of the nephelometer system. To provide meaningful data, the inlet must allow all particles of interest to be collected with the same collection effectiveness independent of sampling conditions in the field environment. These conditions include mean velocity, turbulence scale and intensity, and extraneous airborne matter.

Principal investigator and personnel of the Aerosol Science Laboratory have designed, developed and reduced to practice several versions of Ambient Aerosol Inlet during the past decade. These devices have been exhaustively laboratory and field tested. A review article on ambient aerosol sampling has been published by the principal investigator [45]. At the present time, there are two basic approaches to the sampling of atmospheric particulate matter: the Hi-Vol and the dichotomous samplers. The Wedding PM₁₀ inlet developed for the dichotomous sampler [11], which collects two samples separated into fine and coarse (>2.5 μm) particle modes, will be used as the sampling inlet for the proposed nephelometer system. The inlet is illustrated in Figure 3. It employs an omnidirectional cyclone fractionator, allowing the aerosol entry from any angle of approach. An angular impetus is imparted to the particle

motion via the eight evenly spaced entrance vanes. As the particles enter the inlet they follow the fluid stream lines along the lower radius and enter the cyclone fractionator through the vane system. Particle removal is realized on the inner collection tube. The flow with unremoved particles then enters the middle tube, where the trajectory is altered and the flow continues upward. An additional turn is made to alter the flow into a downward trajectory to allow the particles to proceed to the scattering volume.

The Wedding PM₁₀ Inlet is designed to be operated at a sampling flow rate of 16.67 μpm . Effectiveness values, which is defined as a ratio of mass concentration collected by the inlet to that present in the ambient air, have been determined, as shown in Figure 4, through a series of wind tunnel tests at three wind speeds of 2, 8, and 24 km/h. D_{50} value, associated with a 50% effectiveness value, of the Wedding PM₁₀ Inlet is $10.1 \sim 10.7 \mu\text{m}$. Effectiveness value decreases to zero for particles larger than 20 μm . In order to sample larger particles, modification of present inlet to have D_{50} value of 15 μm can be considered as an option in the Phase II work.

A schematic of particle sampling system is illustrated in Figure 5. Particles, after passing through the inlet, are traveling downward inside the inlet exhaust tube. In order to achieve single particle scattering for a high particle concentration, it is necessary to reduce the particle velocity and to dilute the particle cloud. An isokinetic sampling nozzle is placed at the center of the inlet exhaust tube to sample isokinetically a part of particle flow at a flow rate of 1.0 μpm . Outlet flow from the isokinetic sampling nozzle is expanded to reduce the particle velocity. A second isokinetic sampling nozzle is used to draw a

sample into the scattering volume of the optical system. A sheath of filtered clean air is drawn to provide laminar flow condition around the particle flow outcoming from the sampling nozzle. Clean sheath air is also needed to eliminate the background optical noise due to scattering by particles in the beam path outside the viewing volume of the detector optics.

For optional aircraft usage, a bag sampling system, which has been used successfully in particle size measurements with EAA (Electrical Aerosol Analyzer) by many workers [46] is proposed. Real-time measurement is difficult for aircraft measurement because of high flight speed of the aircraft. First the vacuum pump empties the sampling bag to prepare for a new sample. When the bag is completely empty, the operator closes the bag evacuation valve and opens the aerosol inlet valve until the bag is full. A sample of air is drawn through an isokinetic sampler [47] located outside the aircraft boundary layer. He then closes the inlet valve, adjusts the flow rate through the nephelometer system, and begins the measurement cycle.

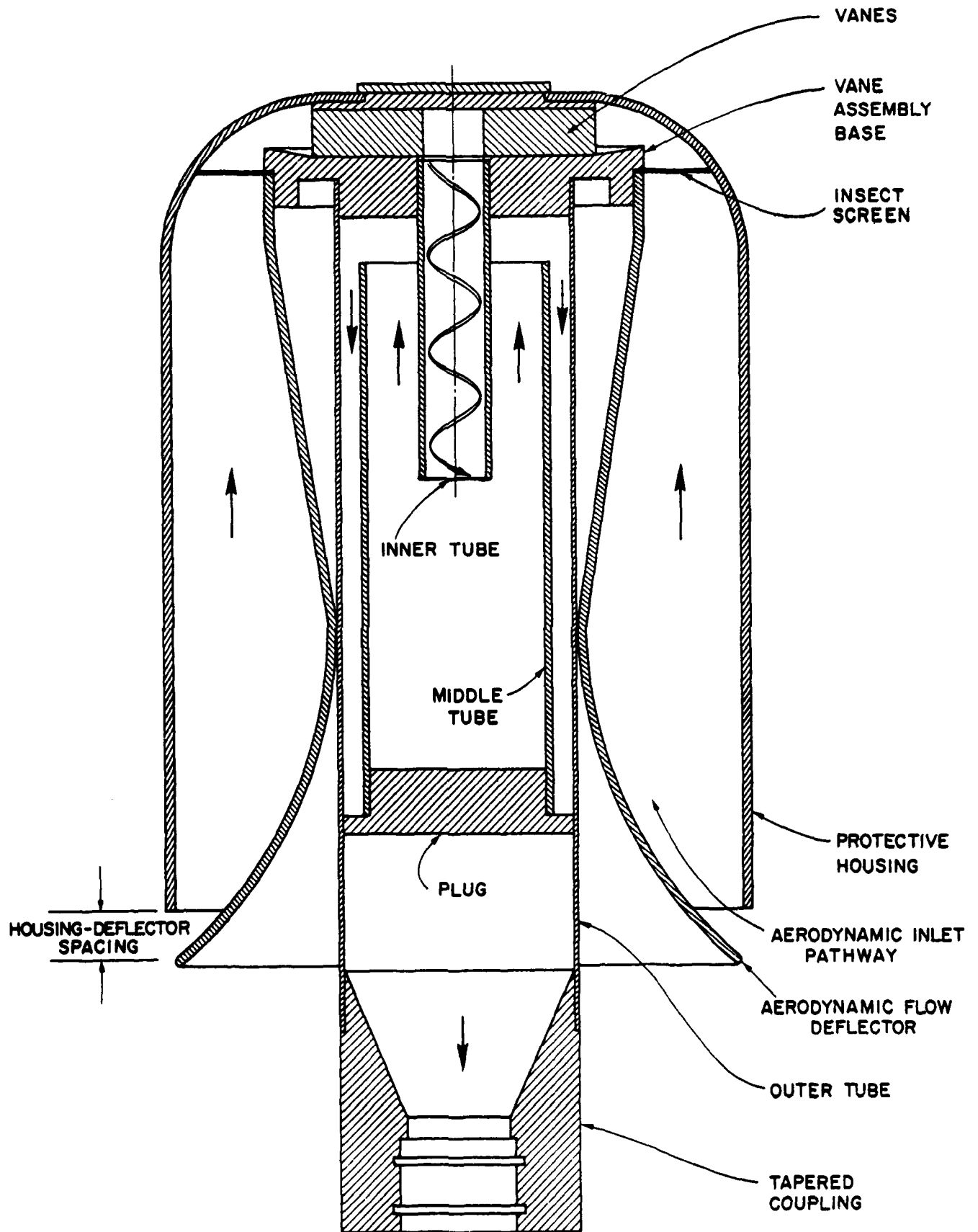


Figure 3
Wedding PM₁₀ Inlet [11]

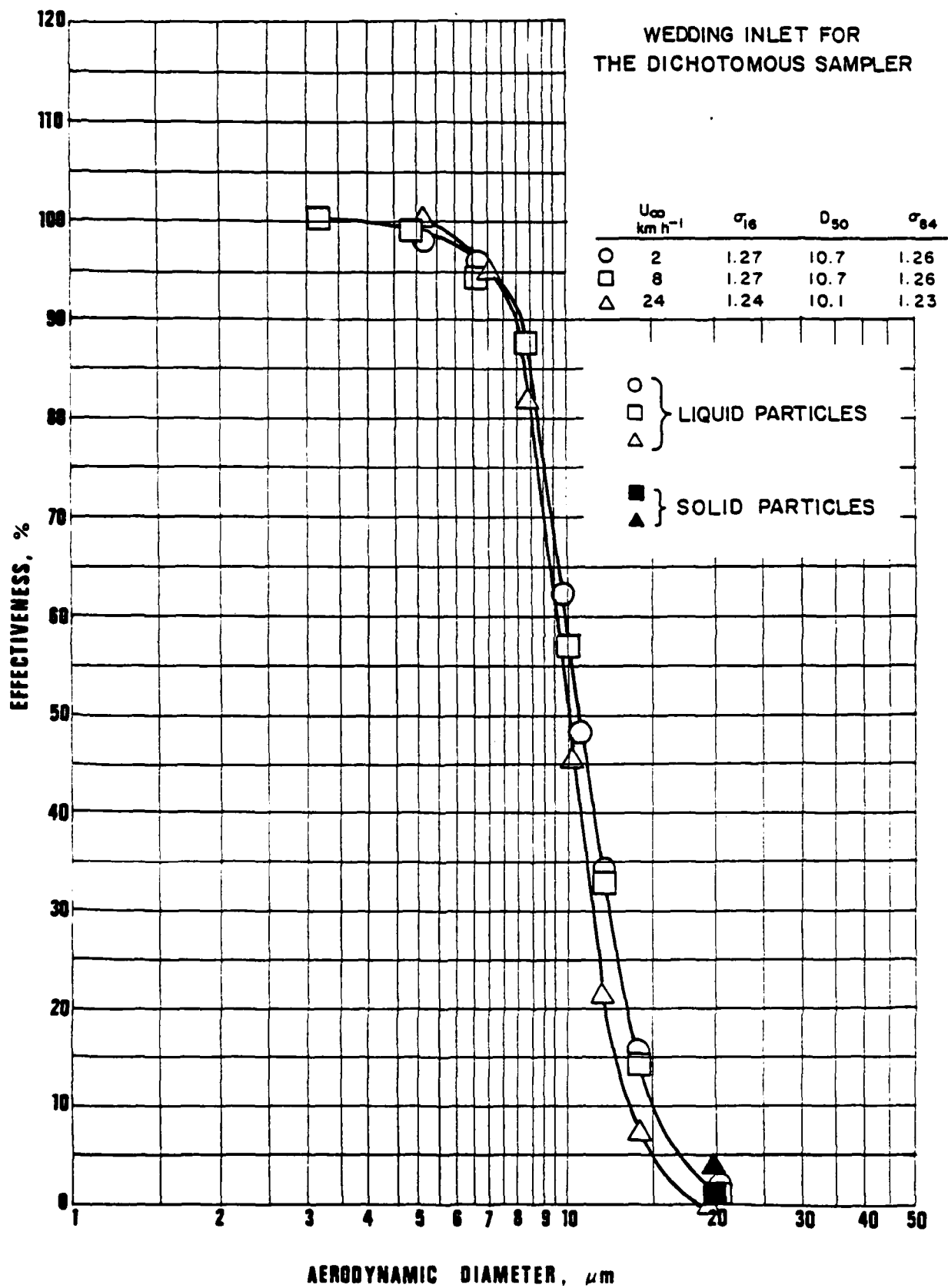


Figure 4
Effectiveness Curve for the Wedding PM₁₀ Inlet

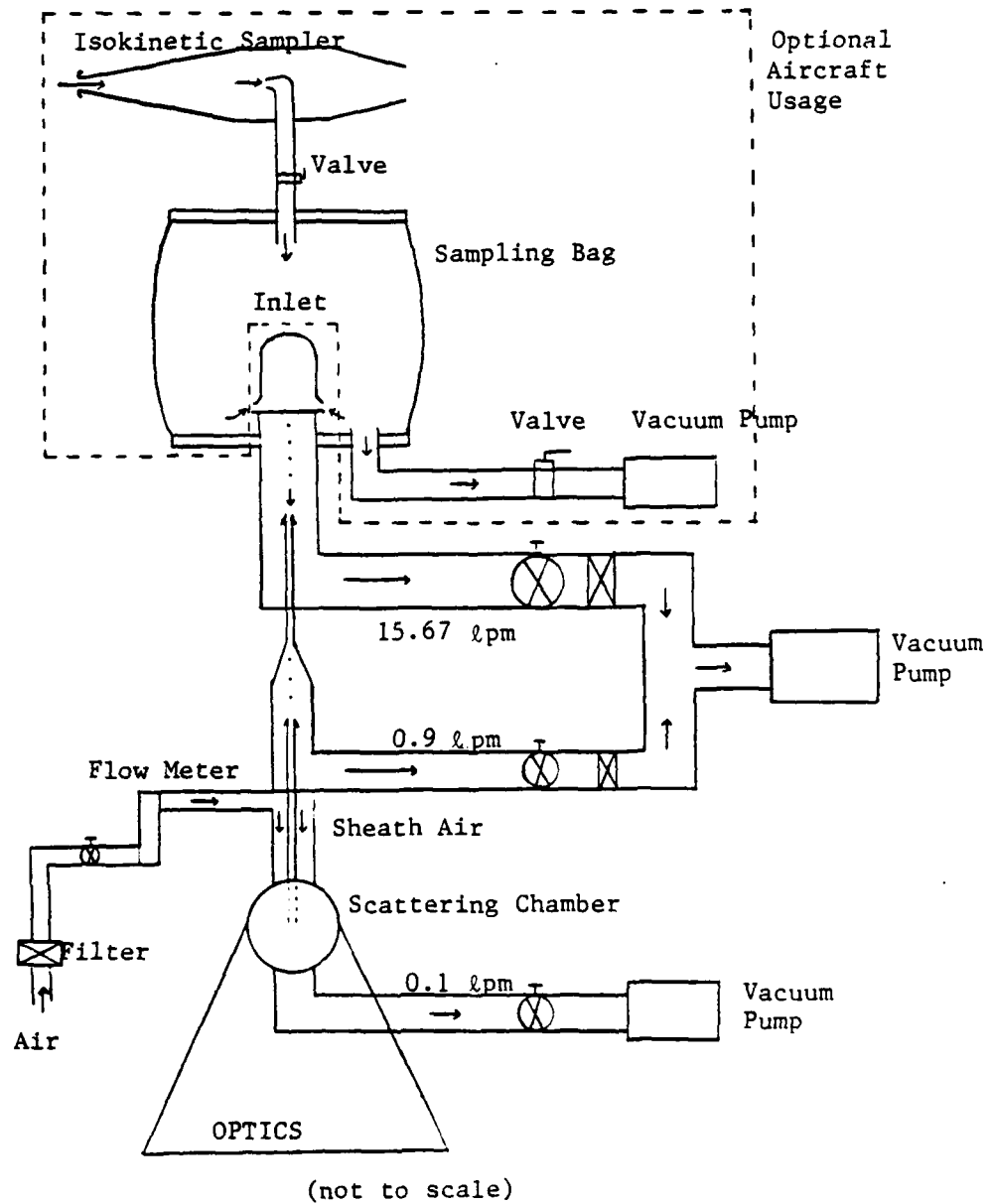


Figure 5
Particle Sampling System

4.3 Optical System

1) Background

Various optical configurations have been reported for single particle differential scattering measurements. In 1961, before lasers were a common laboratory instrument, Gucker and Egan [48] published angular light scattering measurements for single isolated particles. Since the advent of high-power collimated lasers and high speed data acquisition systems, many measurements on single particles have been published particularly in the last decade. To successfully obtain angular light scattering information from single particles it is usually necessary to take one of two approaches: stably suspend the particles and take measurements, or make rapid measurements on single particles in flow. Particle suspension methods can not be used for the proposed nephelometer system because of their slow measurement speed.

Rapid light scattering measurements, during the short time it takes a particle to transit the scattering volume, can be done in two ways: with a rotating detector or aperture (or both), or with an array of fixed detectors. Gucker et al. [49] used a segment of ellipsoidal mirror to direct light scattered by a particle at one focus to a detector fixed at the other focus; an aperture (2° or 5°) rotating at 4000 rpm then gives a 360° scan in 15 msec. Marshall et al. [50] used similar optical system which gives a 360° scan in 20 msec. Morris et al. [51] mounted a detector on a turntable that rotates at 1Hz. Gram et al. [52] developed a laser polar nephelometer for airborne measurements which used a detector rotated by a stepping motor at a frequency of 5Hz. Moser [53] used two conical reflectors and a rotating prism to scan 360° in 4 msec. However, the last two systems measure light scattering by an ensemble of particles.

Fixed detector arrays were devised by Diehl et al. [54], Crowell et al. [55] and Bartholdi et al. [56,57] to measure angular scattering by single particles. Diehl et al. mounted detectors at $\pm 45^\circ$, $\pm 90^\circ$, $\pm 135^\circ$, combinations of either two or three of which sampled scattered light at 16.7 msec intervals. This discrete detector system can not provide enough angular resolution in scattering measurements. Crowell et al. used a photodiode array consisting of 32 concentric rings to measure scattered light intensities simultaneously at 32 forward scattering angles. Approximately 250 μ sec was needed to acquire an event and to transfer its scatter pattern to the computer. The instrument of Bartholdi et al. [57] has an annular segment of an ellipsoidal reflector to focus scattered light onto a circular array of 60 photodiode detectors. This system was designed for applications in which biological cells flow in single file at a flow rate of up to 1000 particles per second through the scattering volume. Optical configuration utilizing a detector array can provide high speed scattering measurements of single particles. However, all systems developed to date measure scattering intensities in one scattering plane at one wavelength.

2) Scattered Radiant Flux Calculation

Expected radiant flux levels incident on the detectors have to be estimated to determine the signal-to-noise ratio and specific detector types to be used. Total radiant flux P_s , scattered into 4π steradian sphere by a single particle can be given by

$$P_s = E_\lambda \frac{\pi D^2}{4} Q_{scat} \quad (7)$$

where E_λ is irradiance incident upon a single particle in the scattering volume. E_λ is determined from $E_\lambda = \frac{4P_o}{\pi w^2}$, where P_o is light source

output power and w is a beam waist diameter. Total scattered radiant flux, P_s values have been calculated based on Q_{scat} values shown in Tables 1-4 for different particle sizes and beam wavelengths, and results are shown in Table 5. Refractive index value of $1.55-0.005i$, which is known to be an average value for atmospheric aerosols [58,59], has been used. The beam waist diameter, w , was assumed to be $100 \mu\text{m}$. Air molecule in the scattering volume also scatters the incident light in all directions, which is Rayleigh scattering. The scattering volume size is inversely proportional to $\sin\theta$. Size of the scattering volume averaged over 4π steradians was assumed to be 10^{-5} cm^3 ; $100 \mu\text{m} \times 100 \mu\text{m} \times 1 \text{ mm}$. Total scattered power levels at three laser wavelengths due to Rayleigh scattering of air molecules in the scattering volume, which are related to the background noise level, are also calculated in Table 5. Because of small beam waist size, background scattering by air molecules is negligible compared to scattering by particles of interest.

Radiant flux values shown in Table 5 are not those actually incident on each detector, which would receive only a small fraction, which is subtended to the detector aperture opening, of total scattered light into 4π sphere. Angular distribution of scattered light also varies with particle size (size parameter) as shown in Figure 1. Power levels which would be incident on detectors located at different scattering angles over 2π degrees have been estimated and presented in Table 6. Solid angle to which each detector subtends was assumed to be 6.99×10^{-3} steradians for $\Delta\theta=3^\circ$ and $\Delta\phi=7.64^\circ$. Total power loss due to non-perfect transmittances/reflectances of optical components throughout the beam path was assumed to be 50% as a conservative estimate.

From Table 6, expected radiant flux values incident on detectors at the scattering angles in the forward to backward directions are found as; $10^{-12} \sim 10^{-7}$ W at 0.6328 μm , $10^{-14} \sim 10^{-7}$ W at 3.39 μm , and $10^{-5} \sim 10^{-14}$ W at 10.6 μm . Typical noise equivalent power (NEP) value of a silicone photodiode is 10^{-14} W/ $\sqrt{\text{Hz}}$. Thus it is feasible for a Si photodetector to measure the angular distribution of scattered light at 0.6328 μm by a single particle in the size range of interest, 0.3 \sim 20 μm . However, in the infrared wavelengths no detector is available for measurement of radiant radiation less than 10^{-11} watts. Low value of expected radiant flux from a single particle scattering at two infrared wavelengths preclude the use of uncooled infrared detectors. NEP of cooled detectors is at the order of $10^{-12} \sim 10^{-11}$ W/ $\sqrt{\text{Hz}}$. Thermoelectrically cooled InAs detector and liquid nitrogen cooled (77°K) HgCdTe detector are chosen for 3.39 and 10.6 μm measurements, respectively. Thus, at the two infrared wavelengths, 3.39 and 10.6 μm , measurement of angular scattering distribution by a single particle is practically limited even with a cooled detector to particles larger than 1.0 μm . However, since the size parameter values of particles smaller than 1.0 μm are less than one at both 3.39 and 10.6 μm wavelengths, scattering by those particles can be considered as Rayleigh scattering which results in same phase function given by equation (5) independent of particle size, shape, and refractive index. There is no need to measure phase function at 3.39 and 10.6 μm wavelengths of particles smaller than 1.0 μm because it is already known from Rayleigh scattering.

Calculations shown in Table 6 were based on scattering of a spherical particle having refractive index of 1.55-0.005i. Particles of different shape and/or refractive index would result in different angular

Table 5

Total Radiant Flux Scattered by a Single Particle, P_s (watts)

Particle Diameter (μm)	P_s		
	$\lambda = 0.6328\mu\text{m}$ ($P_0=25\text{mw}$)	$\lambda = 3.39\mu\text{m}$ ($P_0=25\text{mw}$)	$\lambda = 10.6\mu\text{m}$ ($P_0=3\text{w}$)
0.3	2.01×10^{-7}	3.67×10^{-10}	4.57×10^{-10}
0.6	3.24×10^{-6}	2.38×10^{-8}	2.93×10^{-8}
1.0	8.69×10^{-5}	4.90×10^{-7}	6.32×10^{-7}
3.0	5.12×10^{-4}	8.03×10^{-5}	4.53×10^{-4}
10.0	3.99×10^{-3}	6.47×10^{-4}	1.08×10^{-1}
20.0	1.27×10^{-3}	1.70×10^{-3}	2.65×10^{-1}
Air Molecules	2.21×10^{-10}	2.60×10^{-13}	3.27×10^{-13}

Table 6

Range of Expected Power Incident on a Detector

at $0^\circ \sim 180^\circ$ Scattering Angles, $P_s(\theta)$ (watts)

Particle Diameter (μm)	$P_s(\theta)$		
	$\lambda = 0.6328\mu\text{m}$	$\lambda = 3.39\mu\text{m}$	$\lambda = 10.6\mu\text{m}$
0.3	$5 \times 10^{-11} \sim 2 \times 10^{-12}$	$\sim 10^{-14}$	$\sim 10^{-14}$
0.6	$5 \times 10^{-10} \sim 10^{-11}$	$\sim 10^{-12}$	$\sim 10^{-12}$
1.0	$2 \times 10^{-9} \sim 6 \times 10^{-12}$	$10^{-10} \sim 10^{-11}$	$\sim 10^{-10}$
3.0	$10^{-9} \sim 10^{-12}$	$2 \times 10^{-8} \sim 10^{-10}$	$10^{-7} \sim 3 \times 10^{-8}$
10.0	$10^{-7} \sim 2 \times 10^{-12}$	$10^{-7} \sim 10^{-10}$	$2 \times 10^{-5} \sim 1 \times 10^{-7}$
20.0	$3 \times 10^{-7} \sim 6 \times 10^{-12}$	$4 \times 10^{-7} \sim 10^{-10}$	$6 \times 10^{-5} \sim 2 \times 10^{-7}$

distributions/amplitudes which may not be much different from those presented in Table 6. It is concluded that it is feasible to measure the phase function of a single particle at the proposed three wavelengths; 0.6328, 3.39, and 10.6 μm . Three types of detectors, Si photodiodes, InAs detector, and HgCdTe detector, were chosen for three laser wavelengths, respectively.

3) Optical System

Three different approaches to optical system design of the proposed multi-wavelength, multichannel nephelometer were considered and their feasibility has been investigated during Phase I effort. Those three approaches were:

- I. use a number of discrete detectors located over 2π scattering angles around the scattering planes.
- II. use an ellipsoidal reflector at the scattering plane and detector arrays placed in front of the second focus of the ellipsoidal reflector.
- III. same as II but use a rotating aperture instead of detector array to scan entire scattering angles.

Approach I was initially proposed in Phase I proposal. Optical system is relatively simple and easy to be fabricated. Main problems with this approach are poor angular resolution due to space limitation resulted from actual size of detectors, and incapability of measuring scattered intensities simultaneously at the same scattering angle at three wavelengths. It was concluded from scattering radiant flux calculation in the previous section that three different detectors had to be used to detect angular scattered intensities by a single particle. A detector such as a pyroelectric detector, which has a flat response over the entire spectrum from visible to infrared regions, can not be used. Three detectors have to be placed closely at locations of each scattering angle

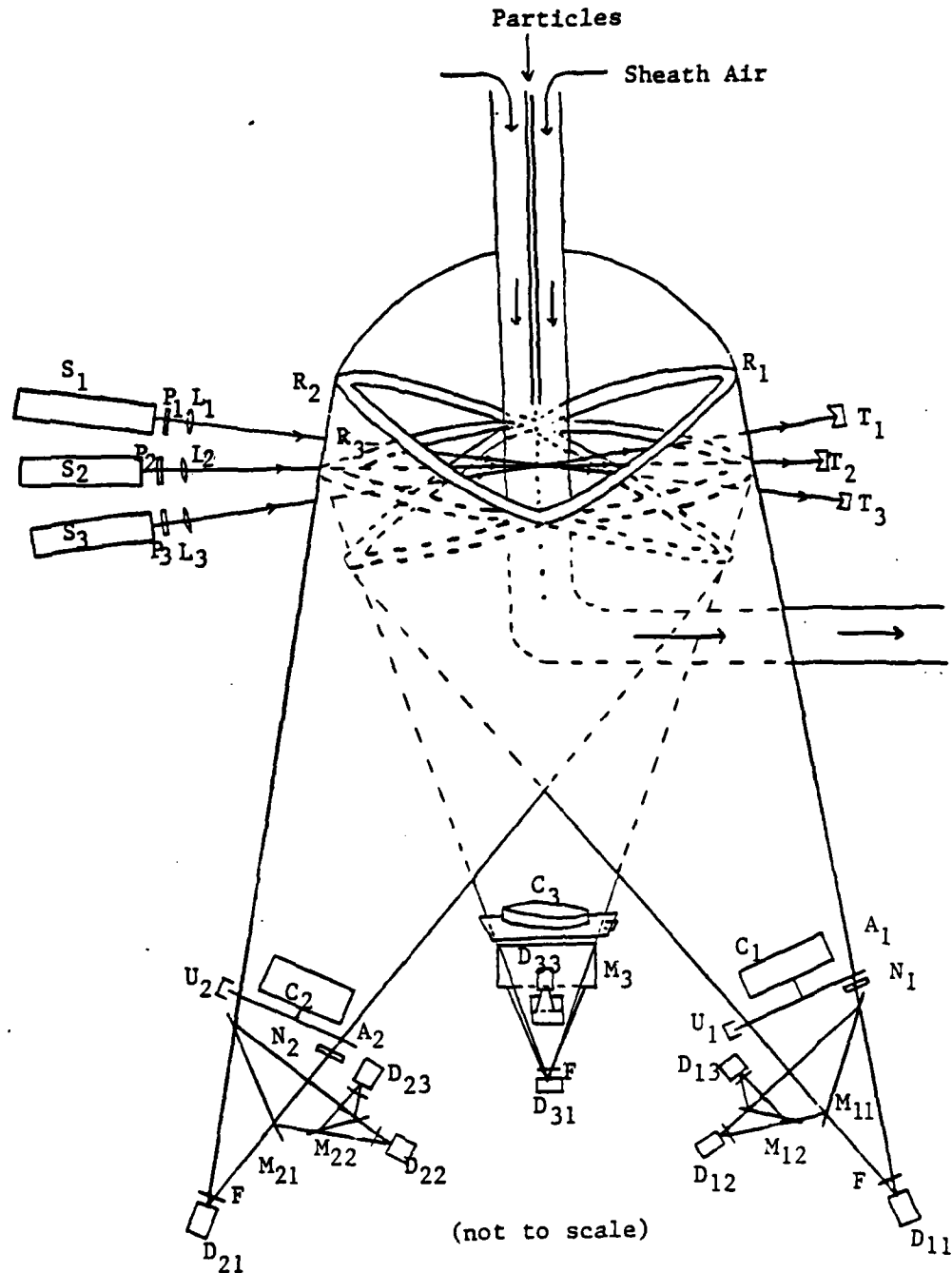
to be measured. Actual size of detectors, especially large size of infrared detectors including cooling devices, preclude the measuring of fine signature of differential scattering pattern for particles of interest. In order to measure scattered intensities at N points over 2π degrees, $3N$ detectors are needed for each wavelength to cover three different scattering planes to characterize optical properties of nonspherical particles. In an economic point of view, infrared detectors are expensive so that total cost of the system rises rapidly as one increases N . If N is assumed to be 20, which is certainly not enough to unfold fine shape of angular scattering patterns of a particle over 2π degrees, cost for the total number of detectors would be \$390,000. Another drawback of this approach is that it is impossible to measure the scattered intensities at a same scattering angle for three laser wavelengths. This makes it difficult to investigate dependence of differential scattering pattern on wavelengths when analyzing data measured with the nephelometer. Thus the first approach was withdrawn.

The second approach is to use an ellipsoidal reflector and detector arrays, which is similar to the system employed by Bartholdi et al. [57]. Laser beams intersects the particle flow at the primary focal point of a circular strip of an ellipsoidal reflector. The scattered lights are reflected by the ellipsoidal reflector and directed onto a circular array of detectors placed in front of the secondary focal point. Each detector element senses signals emanating from a region on the strip corresponding to a range of scattering angles. The size and positions of the detector elements determine the angular resolution of the differential scattering pattern. Advantages of using this approach are seen that it is capable of measuring the differential scattering patterns in very fine angular resolution, and in a real-time manner with a high speed data acquisition

system. Only one array is needed for each wavelength per scattering plane to scan over 2π scattering angles. A circular array of 50 detector elements, whose element size is $200 \times 200 \mu\text{m}$ square, around a 0.25" diameter circle was considered. Circular array of photodiodes for measurement at visible wavelength is commercially available. However, for two infrared wavelengths the circular detector arrays have to be custom-made ones. Several leading manufacturers of infrared detectors have been contacted to assess the feasibility of fabricating such detector arrays. It was found that it is technically feasible to fabricate such circular array detectors but cost would be quite expensive. A total of six infrared circular array detectors are needed for two wavelengths measurements at three scattering planes. A very fast, sophisticated data acquisition system is needed to measure and store the differential scattering data signals from 450 detector channels in real-time mode. A powerful, high speed computer similar to the HP1000 system has to be used to do such a job. Signal conditioning electronics including preamplifier, logarithmic amplifier, and peak-sense electronics is also needed at each detector channel output to interface with the input of the data acquisition system. Total equipment/parts cost of a nephelometer employing such optical configuration was estimated to be about \$550,000. With this system sampling rate over 1,000 particles/sec can be accomplished. This approach is technically feasible and can provide fast, real-time measurement of differential scattering patterns in a fine angular resolution at three wavelengths. However, because of its extremely high cost of system equipment, the third approach was considered.

The third approach is to use a rotating aperture instead of a detector array to scan over 2π scattering angles. A schematic of optical system of this approach is shown in Figure 6. A rotating aperture is placed in front of detectors located at the secondary focal point of each ellipsoidal reflector. The size of aperture limits the angular resolution, $\Delta\theta$, of differential scattering measurement. The aperture is mounted on the shaft of a fast scanning motor. Continuous scan measurements over 2π degrees are possible with only one detector for each wavelength per one scattering plane. Thus, a total of nine detectors are needed and this also simplifies performance requirements of the data acquisition system. In this approach, motor speed has to be fast enough to complete a scan over 2π degrees when a particle is still moving inside the scattering volume. The particle sampling system discussed in Section 4.2 was designed to have a particle pass through the scattering volume in about 3 msec. A very fast precision scanning motor which can be driven up to 60,000 rpm is available. The motor will be rotated at a reduced speed of 30,000 rpm, with which it will take 2 msec to complete one scan over 2π degrees. Thus, a 2 msec long pulse emanates from each detector output when a particle passes through the scattering volume. A differential scattering pattern of that particle can be obtained by sampling and digitizing that pulse with a certain time increment. Total acquisition/conversion time required by the analog-to-digital converter of the data acquisition system is $10 \mu\text{sec}$, which means a maximum of 200 samplings over 2π degrees is possible. Fifty samplings over 2π degrees with angular resolution of 3° , which is determined by the aperture size, is proposed. Sampling rate attainable with this approach is lower than that of detector array approach, but maximum sampling rate of 500 particles/sec is still higher than the system requirement which is 100

Figure 6
Optical System



A_i : Rotating Apertures
 C_i : Scanning Motors
 D_{ij} : Detectors
 F_i : Interference Filters
 L_i : Focusing Lenses
 M_{ij} : Hot Mirrors

N_i : Neutral Density Filters
 P_i : Polarizers
 R_i : Ellipsoidal Reflectors
 S_i : Lasers
 T_i : Light Traps
 U_i : Photosensitive Pick-ups

particles/sec. One problem with this approach is that the particle keeps moving in the scattering volume while the aperture scans over 2π degrees angles. The particle's rotational motion in a time period of 2 msec can be neglected under the laminar flow condition. Intensity distribution of focused laser beam across the scattering volume has a gaussian shape. Change in scattered intensity due to uneven distribution of incident beam intensity across the scattering volume will be corrected through experimental calibration of the system with monodisperse spherical particles of known size and refractive index and numerical analysis of the measured data. Because of the system's simplicity and economical reasons, the third approach employing rotating apertures has been finally chosen for the optical system of the proposed multi-wavelength, multi-channel nephelometer system.

Three lasers; a 25mW, 0.6328 μm HeNe laser, a 25mW, 3.39 μm HeNe infrared laser, and a 3W, 10.6 μm CO₂ laser, are chosen as light sources. Instead of a 1.06 μm Nd-YAG laser, an infrared HeNe laser emitting 3.39 μm radiation is chosen because 3.39 μm falls in the atmospheric window region of 3~5 μm where many infrared systems are operated. Another reason is the CW Nd-YAG laser is bulkier than the HeNe laser because it needs a cooling system. If the 1.06 μm laser is used, a photodiode can be used as a detector and differential scattering of submicron particles can also be measured. A sealed tube type CO₂ laser is chosen for the same reason, although it needs a cooling system and a cooled detector, because its wavelength is in the 8~12 μm atmospheric window region and it is widely used in many infrared applications. A portable heat exchanger will be used as a cooling system for the CO₂ laser. Other lasers such as the He-Cd laser (0.442 μm), Argon ion laser (0.488 or 0.515 μm) and turnable dye laser (0.4~0.9 μm) were also considered as light sources. Use of

three visible or near infrared (1.06 μm) lasers could allow employment of the circular array detector approach and reduce the system complexity. However, one of the important objectives of the proposed nephelometer development is to measure the optical properties of atmospheric aerosols over a wide spectrum range from visible to far infrared wavelengths. That justifies the choice of two infrared lasers emitting 3.39 and 10.6 μm .

Three laser beams are focused with lenses onto the scattering volume at the primary focal points of ellipsoidal reflectors. Anti-reflection coated ZnSe lenses are used to focus two infrared laser beams. Because of the refractive index change of the optical material with wavelength, one coaxial beam approach consisting of three wavelengths can not be used. Each of three laser beams is focused with its matching lenses onto the same spot at the scattering volume using fine alignment adjustments.

Three angular segments of ellipsoidal reflectors are mounted along three scattering planes around a sphere centered at the scattering volume. Light beams scattered by a particle at the scattering volume are reflected by ellipsoidal reflectors and directed through the rotating apertures onto detectors located at the secondary focal points. A photosensitive pickup is mounted across the aperture plate at zero scattering angle position. Its output, which is used to synchronize scanning procedure of differential scattering measurement, is connected to the data acquisition system.

After passing through the aperture, scattered beams consisting of three wavelengths are separated into three wavelength components using ZnSe hot mirrors. In front of each detector is an interference filter which prevents stray radiation from reaching the detector surface.

Polarizers will be placed in removable mounts located in front of lasers and detectors. Neutral density filters will be inserted at the forward scattering positions to reduce the beam intensity incident on the detectors. All optical beam paths are enclosed in housings to keep the background radiation level as low as possible. Three types of detectors will be used; Si photodiode for 0.6328 μm , thermoelectronically cooled (195°K) InAs detector for 3.39 μm , and a liquid nitrogen cooled (77°K) HgCdTe detector for 10.6 μm . Typical specifications of these three detectors are shown in Table 7.

Table 7
Typical Specifications of Detectors

	<u>Si Photodiode</u>	<u>InAs</u>	<u>HgCdTe</u>
sensitive wavelength (μm)	0.18~1.15	1.0~3.8	2~14
peak wavelength (μm)	0.85	3.2	10.6
responsivity (A/W)	0.55	1.0	3 30
NEP (W/ $\sqrt{\text{Hz}}$)	6×10^{-14}	-	-
detectivity, D^* ($\text{cmHz}^{\frac{1}{2}} \text{W}^{-1}$)	-	1.0×10^{11}	2×10^{10}
operating temperature (°K)	ambient	195	77
cooling	-	4-stage TE cooler	liquid N ₂

4.4 Data Acquisition System

A high speed, computer-based signal processing and data acquisition system, which can sample nine detector channel outputs, measure their amplitudes, and store measured values in the memory, is needed. A 2 msec long differential scattering pulse from each of nine detectors has to be sampled at least 50 times and a maximum of 100 particles have to be sampled in one second. Thus, total sampling rate is 45,000 samples/sec. All these measured data have to be continuously stored on a memory storage device at a transfer rate of 90K bytes/sec, assuming each data consists of two bytes. Sampling nine channels at 25KHz per channel requires a total aggregate sampling rate of 225 KHz. A high-performance, computer-based data acquisition, which is capable of analog acquisition to memory at up to 250,000 samples-per-second and continuous analog throughput to or from disk at up to 100,000 samples-per-second, has been designed. A schematic of the data acquisition system is shown in Figure 7. The system is based on the LSI-11/23 microcomputer CPU, with EIS (Extended Instruction Set), FPU (Floating-point Processing Unit), MMU (Memory Management Unit), 256K Bytes memory, and a real-time clock.

Each detector output is amplified with a matching preamplifier and filtered with a bandpass filter to improve signal quality. Logarithmic amplifiers are used to increase the dynamic range of measurement system and improve system resolution for low-level signals. Scattered radiant flux calculations in section 4.1 showed orders of magnitude change in differential scattering data. Conventional method using a multiplexer to scan multi-channel inputs is not suitable for the present nephelometer application. Ideally, one has to sample nine channels at exactly the same moment to get scattered intensity values corresponding to same scattering angle. Unavoidable time delay between each conversion when using a

conventional multiplexer makes simultaneous measurements impossible. To solve this problem, a simultaneous sample and holding (SS&H) circuit is used at the analog input stage of the data acquisition system. This method lets the circuit acquire nine analog input signals using nine separate sample and hold circuits, which switch between sampling and holding simultaneously to within ± 5 ns. Thus, the SS&H circuit takes a snapshot of nine analog input channels, freezing their values within a ± 5 nanosecond aperture uncertainty interval. Subsequent analog to conversions with 12-bit resolution occur at up to 250 KHz throughput rate.

The gathering of data with a microcomputer based data acquisition system has been limited traditionally either to slow data rates less than 10 KHz aggregate or to small quantities of data points fewer than 16,000 samples. Attempts to gather large numbers of samples at aggregate rates greater than 10 KHz have resulted in data files which contain gaps or discontinuities of an indeterminate nature. In a typical system, data is output directly from a high performance DMA (Direct Memory Access) A/D interface to memory and subsequently rewritten from memory to disk. Memory is typically organized as two buffers so that while one buffer is being filled, the other buffer is being emptied to disk. Each word of data is transferred over the system bus twice, once from the A/D to memory and once from memory to disk. When the data acquisition rate is greater than 10 KHz, data are lost between buffers. A dual ported data acquisition architecture is used in Figure 7 to remove this constraint. The external path connecting two boards allows the A/D board to send data to memory without using the processor bus; the system bus is needed only to transfer data from memory to disk. The dual port RAM board includes a dual channel, On-board Address Controller (OAC) which allows the memory to

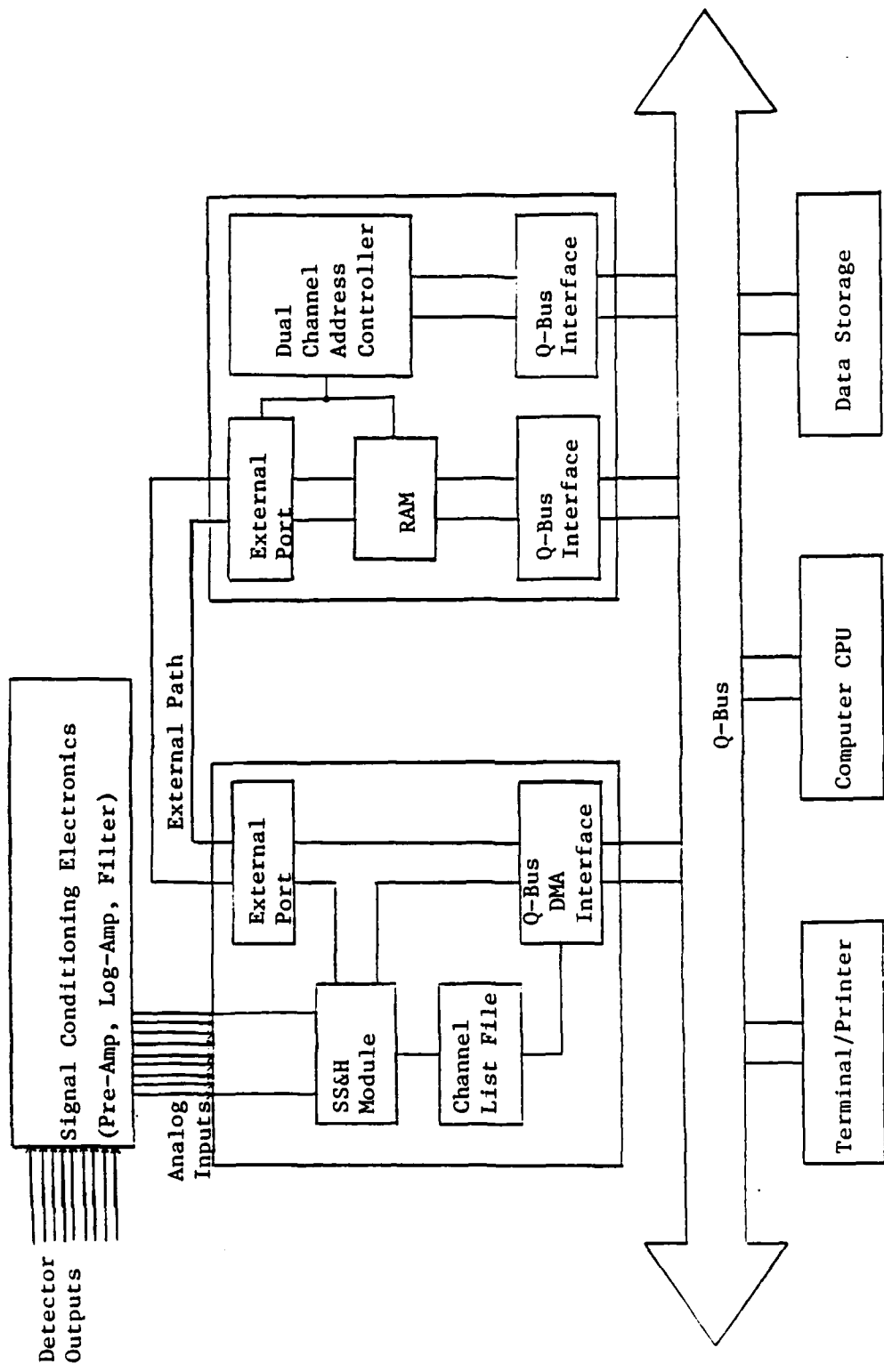


Figure 7
Data Acquisition System

be configured as two separate buffers. The OAC can be set up to alternate between two separate buffers. The memory buffers are sufficiently large and the buffer control logic is sufficiently fast so that this buffer switching process, known as channel chaining, can be continued indefinitely, without loss of any A/D data points, at rates up to 1 MHz, subject to the transfer rate limits of the A/D device, the processor bus, and the mass storage subsystem.

The data acquisition system includes two mass-storage devices, a floppy/hard disk drive which provides 1 Mbytes of diskette storage and a 35.6 Mbytes Winchester hard-disk drive. Hard-disk drives are needed to store measured data at a high transfer rate in a real-time manner. 35.6 Mbytes of data is equal to differential scattering data of as many as 3,955 particles. Since the disk in the Winchester drive can not be removed, a 60 Mbytes cartridge tape drive, which is much slower than hard-disk drive, is used as a back-up device for permanent storage of measured data. Once the disk in the Winchester drive is filled with data words, measurement stops and the stored data are dumped to the cartridge tape for future data analysis. Other auxiliary devices of the data acquisition system are a video terminal and a dot-matrix printer.

The system software includes RT-11 operating system, FORTRAN compiler, and CPLIB and DTLIB subroutine packages. CPLIB and DTLIB support analog input/output, transfer of data, hardware interfaces, and high resolution plotting. CPLIB and DTLIB consist of a library of subroutines designed to be linked to user FORTRAN programs and operated under RT-11 real-time operating system.

5.0 Potential Post Applications

5.1 Potential Commercial Applications

Potential commercial applications of the proposed multi-wavelength, multichannel nephelometer are seen for researchers and engineers in the field of:

(1) Health Effects and Environmental Instrumentation:

1.1 Air quality monitoring; Inhalable particulate matter whose size is less than 15 μm are important for health effects analysis because these particles deposit in the tracheo-bronchial and alveolar regions of the human respiratory tract. Information on the size distribution of ambient airborne particles in that size range is of great importance in assessing air quality and health effects.

1.2 Visibility degradation; Absorption and scattering of lightwaves by particulates in the atmosphere is one of the major mechanisms causing degradation of atmospheric visibility. Characterization of optical properties of atmospheric particles with the proposed nephelometer system will enhance ones ability of understanding effects of atmospheric particles on visibility degradation.

(2) Medical and Biological Research;

Optical analysis of the biological cells is a valuable tool in medical and biological research. Light scattering technique can be used for the rapid, quantitative analysis of individual microscopic objects, such as biological cells. Morphology of cells can be classified from differential light-scattering data measured with the proposed nephelometer system.

(3) Chemical and Process Engineering;

3.1 On-Line characterization of irregularly shaped suspended particles in multi-phase and multi-component system; Optical particle sizing instruments available at present give erroneous results for non-spherical particles. Measurements of an entire differential scattering pattern of individual particles with the proposed nephelometer will provide more accurate information on size and shape of suspended particles,

3.2 Combustion process analysis; In-situ measurements of particle loading and size distribution can provide important data for the reliable design of combustion process equipment and control of environmental factors. Examples of current and potential applications of the proposed nephelometer include the study of: ash formation from pulverized coal, mineral carry over from fluidized bed combustors and pressurized gasifiers, droplet formation and distribution in spray combustors, and radiative heat transfer.

(4) Radiation Transfer and Atmospheric Optics:

The presence of suspended particulate matter in the atmosphere modifies the solar radiation reaching the earth, due to both scattering and absorption. Characterization of optical properties of atmospheric aerosols with the proposed nephelometer will provide valuable information needed to develop models describing the radiative energy exchange in the earth-atmosphere system, and the effects which the addition of aerosols has on this exchange. Quantitative analysis of atmospheric scattering phenomena are often limited by the fact

that little information is available about refractive index values. Differential scattering data can be used to determine the complex index of refraction of airborne particles.

(5) Optical Particle Sizing:

Optical particle sizing instruments developed to date give erroneous results for nonspherical particles application. Based on the knowledge obtained from measurements with the proposed nephelometer, development of a new instrument, which can provide an in-situ measurement of particle size of nonspherical particles, can be directed.

5.2 Potential Use by the Federal Government

Potential uses of the multi-wavelength, multichannel nephelometer system developed through the proposed project are expected in the field of:

(1) Performance Analysis of Optical and Infrared Systems;

Performance of optical/infrared systems such as: thermal imaging system, night vision devices, FLIR system, guidance/seeker, laser rangefinder, laser designator, optical communication, and directed energy weapon system is greatly affected by atmospheric conditions under which those systems have to be operated. Characterization of optical properties of atmospheric aerosols with the proposed nephelometer will enhance one's ability to predict EO/IR systems performance under different atmospheric conditions.

(2) Optical Countermeasures:

Characterization of optical properties of aerosol particles will provide an understanding of principles governing the optical merit of obscurants. Effectiveness of optical countermeasures such as

obscurant smokes can be analyzed based on the phase function data measured with the proposed nephelometer.

(3) Chemical/Biological Agent Detection;

Correlation of particle optical properties measured with the proposed nephelometer with known chemical and/or biological constituents will greatly advance the development of CB agent detection system.

(4) Atmospheric Modeling of Optical/Infrared Radiation Transmissions

Characterization of optical properties of atmospheric aerosols can provide a data base for an attempt to model and predict their effects on the propagation of optical and infrared radiation. These effects include transmission loss, contrast degradation, and path radiance. Optical paths through the atmosphere include horizontal and/or slant paths.

(5) Remote Sensing

Knowledge on the optical properties of aerosol particles will greatly enhance ones ability to interpret the experimental data measured with remote-sensing instruments such as multi-wavelength solar radiometer, monostatic and bistatic lidars, and imaging systems.

6.0 Conclusions

Design parameters for a multi-wavelength, multichannel nephelometer system, which is capable of measuring differential scattering patterns of individual aerosol particles, have been optimized. System design includes the particle sampling inlet, the optical system, and the data acquisition system. The new system provides means for making in-situ, real-time, multi-wavelength measurements of the optical properties of individual aerosol particles of different shape and composition. The system uses 0.6328, 3.39, and 10.6 μm laser wavelengths, which are in the visible and infrared atmospheric window regions. The optical system measures multi-wavelength differential scattering patterns of a single particle in three different scattering planes to account for effects of particle orientation on scattering by nonspherical particles. The particle sampling inlet/system samples particles with minimal dependence on the micrometeorological conditions of the ambient atmosphere and directs them in a train of single particles into the scattering volume. The computer-based data acquisition system can acquire the measured differential scattering data and store them simultaneously into a mass storage device without any data loss.

The Phase II research and development effort involves fabrication, calibration and performance testing of the multi-wavelength, multichannel nephelometer based on the specific design of the system resulting from the Phase I research work. This new nephelometer system, if it is developed successfully during the Phase II effort, will be able to provide information which can enhance one's knowledge concerning the optical properties of airborne particles. If this knowledge is obtained, then the ability to predict performance of optical and infrared systems through the atmosphere is enhanced. The uniqueness of this approach lies in the inherent ability of the system to produce data heretofore unattainable.

The benefits resulting from the successful development of such an instrument are seen in numerous areas of military and civilian applications. In general, researchers and system designers will have an instrument which will provide more information than presently available with respect to optical/physical properties of individual atmospheric and/or artificial particles. Upon completion of development and performance testing of a prototype of the proposed nephelometer system during Phase II effort, commercial application of such a system will be initiated during Phase III effort.

7.0 Participating Professional Personnel

FAME Associates, Inc. members who participated in Phase I research effort are listed below:

James B. Wedding, Ph.D., Principal Investigator

Young J. Kim, Ph.D., Senior Research Engineer

Michael A. Weigand, Director, Aerosol Science Laboratory

None of the project staff earned advanced degrees during the course of the project.

REFERENCES

1. McClatchey, R. A., et al (1973). AFCRL-TR-73-0096, Air Force Geophysics Lab., Hanscom, MA.
2. Selby, J. E., et al. (1973). "Atmospheric Transmittance/Radiance: Computer Code LOWTRAN5" AFGL-TR-80-0067, Air Force Geophysics Lab., Hanscom MA.
3. McClatchey, R. A. (1979). "Atmospheric Transmission Models and Measurement", SPIE Proceedings, Vol. 195, 2.
4. Duncan, L. D. and Skirkey, R. D. (1983). Optical Engineering, 22, 20.
5. Lin, C. I. et al. (1973). Appl. Opt., 12, 1356.
6. Rosen, H. et al. (1978). Appl. Opt., 17, 3859.
7. van de Hulst, H. C. (1957). Light Scattering by Small Particles, John Wiley and Sons, NY.
8. Kerker, M. (1969). The Scattering of Light and Other Electromagnetic Radiation, Academic Press, New York.
9. Thompson, R. C. et al. (1980). Appl. Opt., 19, 1323.
10. Stuebing, E. W. (1982). SPIE Proceedings, Vol. 305, 2.
11. Wedding, J. B., Weigand, M. A., and Carney, T. C. (1982). Environ. Sci. & Technol., 16, 602.
12. Perrin, F. (1942). J. Chem. Phys., 10, 415.
13. Dave, J. V. (1968). IBM Report 320-3237, IBM Palo Alto Scientific Center, Palo Alto, CA.
14. McCartney, E. J. (1976). Optics of the Atmosphere, John Wiley & Sons, N.Y.
15. Bohren, C. F. and Huffman, D. R. (1983). Absorption and Scattering of Light by Small Particles, John Wiley & Sons, N.Y.
16. Hodkinson, J. R. and Greenleaves, I. J. (1963). J. Opt. Soc. Am., 53, 577.
17. Wait, J. R. (1955). J. Phys., 33, 189.
18. Cohen, L. D. et al. (1983). Applied Optics, 22, 742.
19. Asano, S. and Yamaoto, G. (1975). Applied Optics, 14, 29.
20. Asano, S. and Sato, M. (1980). Applied Optics, 19, 962.
21. Weil, H. and Chu, C. M. (1980). Applied Optics, 19, 2066.
22. Birkhoff, R. D. et al. (1977). J. Opt. Soc. Am., 67, 564.
23. Wiltzius, P. (1982). Applied Optics, 21, 2022.
24. Jones, A. R. (1979). J. Phy. D., 12, 1661.
25. Latimer, P. and Wamble, F. (1982). Applied Optics, 21, 2447.
26. Harrington, R. F. (1968). Field Computation by Moment Method, McMillan, New York.
27. Yeh, C. (1964). Phys. Rev., 135, A1193.
28. Oguchi, T. (1973). Radio Science, 8, 31.
29. Waterman, P. C. (1965). Proc. IEEE, 53, 805.
30. Barber, P. and Yeh, C. (1975). Applied Optics, 14, 2864.
31. Wang, D. and Barber, P. (1979). Applied Optics, 18, 1190.
32. Pollack, J. B. and Cuzzi, J. N. (1980). J. Atmos. Sci., 37, 868.
33. Schuerman, D. W. (ed) (1980). Light Scattering by Irregularly Shaped Particles, Plenum Press, NY.
34. Barber, P. W. and Massoudi, H. (1982). Aerosol Science & Technology, 1, 303.
35. Hodkinson, J. R. (1966). Aerosol Science, C. N. Davies, Ed., Chapter 10, Academic Press, New York.
36. Pinnick, R. G. et al (1976). Applied Optics, 15, 384.

References (cont'd)

37. Holland, A. C. and Gagne, G. (1970). Applied Optics, 9, 1113.
38. Zerull, R. H. and Giese, R. H. (1974). Planets, Stars, and Nebulae Studies with Photopolarimetry, T. Gehrels, Ed., Univ. of Arizona Press.
39. Zerull, R. H. et al. (1977). SPIE vol. 112, Optical Polarimetry, 191.
40. Schuerman, D. W. et al. (1981). Applied Optics, 20, 4039.
41. Born, M. and Wolf, E. (1964). Principles of Optics, McMillan, New York.
42. Gram, G. W. et al. (1974). J. Appl. Meteorol., 13, 449.
43. Reagan, J. A. et al. (1980). J. Geophys. Res., 85, 1591.
44. Farmer, W. M. (1982). "A Calibration Study of the Response Characteristics of the Climet Particle Size Analyzer and the Aerosol Photometer", Final Report for DAAD05-80-C-0026, Univ. of Tennessee Space Institute, Tullahoma, TN.
45. Wedding, J. B. (1982). Environ. Sci. & Technol., 16, 154.
46. Sem, G. J. (1979). in Aerosol Measurement, ed. by Lundgren et al, P. 400, Univ. Press of Florida, Gainesville, FL.
47. Pena, J. A. et al. (1977). J. Air Pollution Control Assoc., 27, 337.
48. Gucker, F. T. and Egan, J. J. (1961). J. Colloid Sci., 16, 68.
49. Gucker, F. T. et al. (1973). J. Aerosol Sci., 4, 389.
50. Marshall, T. R. et al. (1976). J. Colloid & Interface Sci., 55, 624.
51. Morris, S. H. et al. (1979). Appl. Opt., 18, 303.
52. Gram, G. W. et al. (1975). Optical Eng., 14, 85.
53. Moser, H. O. (1974). Appl. Opt., 13, 173.
54. Diehl, S. R. et al. (1979). Appl. Opt., 18, 1653.
55. Crowell, J. U. et al. (1978). IEEE Trans. Biomed. Eng., 25, 519.
56. Bartholdi, M. et al. (1977). Optics Letters, 1, 223.
57. Bartholdi, M. et al. (1980). Appl. Opt., 19, 1573.
58. Grams, G. W. et al. (1974). J. Appl. Meteorol., 13, 459.
59. Bhardwaja, P. S. et al. (1974). Appl. Opt., 13, 731.
60. Berglund, R. N. and Liu, B. Y. H. (1973). Environ. Sci. & Technol., 1, 147.
61. Grams, G. W. (1983). Final Report for DAAG29-79-C-0092, Georgia Institute of Technology, Atlanta, Georgia.
62. Middleton, W. E. K. (1952). Vision Through the Atmosphere, University of Toronto Press.
63. Winstanley, J. V. and Adams, M. J. (1975). Applied Optics, 14, 2151.
64. Gibson, F. W. (1976). Applied Optics, 15, 2520.
65. Ahlquist, N. C. and Charlson, R. J. (1969). Atmospheric Environment, 3, 551.
66. Waggoner, A. P. and Charlson, R. J. (1977). EPA Ecological Series, NTIS Report PB269944.

END

FILMED

10-85

DTIC